Fluorospectroscopy of Dye-Loaded Liposomes in Photonic Crystal Fibers

Yong, Derrick; Lee, Elizabeth; Yu, Xia; Chan, Chi Chiu

2016

Yong, D., Lee, E., Yu, X., & Chan, C. C. (2016). Fluorospectroscopy of Dye-Loaded Liposomes in Photonic Crystal Fibers. IEEE Journal of Selected Topics in Quantum Electronics, 22(3), 1-6.

https://hdl.handle.net/10356/81405

https://doi.org/10.1109/JSTQE.2015.2479919

Fluorospectroscopy of Dye-loaded Liposomes in Photonic Crystal Fibers

Derrick Yong, Elizabeth Lee, Xia Yu, *Senior Member, IEEE*, and Chi Chiu Chan, *Member, IEEE*

***Abstract*—The immobilization and probing of liposomes within photonic crystal fibers was demonstrated for the first time. A bioactive surface was used to tether the liposomes. This bioactive surface consisted of streptavidin bound to a photochemically functionalized biotin layer. Bound streptavidin hence enabled the further binding of biotinylated dye-loaded liposomes. In-fiber fluorescence spectroscopy was used to quantify the streptavidin coverage density. The same method was also used to characterize the surface-tethered liposomes. The further observation of a unique phenomenon – photobleaching dequenching – was used for the first time as an indication of liposomal content retention. This indicated no rupturing of liposomes, highlighting them as bio-derived analogues to dye-doped nanoparticles. The demonstrated integration of liposomes with optical waveguides shows potential as a bio-integrated photonic device.**

***Index Terms*—Fluorescence spectroscopy; Liposomes; Photochemistry; Photonic crystal fibers.**

I. Introduction

THE myriad of advances in the field of fiber optic technology has been realized by the advent of photonic crystal fibers (PCFs) [1, 2]. Their periodic arrays of microstructured air holes, provide not only a means of light guidance, but further serve as infiltratable microfluidic channels for in-fiber light-matter interactions. This has led to a multitude of applications that have been widely reviewed [3-6]. In more recent years, PCF applications have evolved to better harness their integrated optics and fluidic traits. Primarily, this entailed the use of PCFs as micro- or nano-reactors for the in-fiber monitoring and generation of photochemical or photocatalytic processes [5, 7-10] – boasting infinitesimal volume requirements and vastly superior interaction lengths in contrast to conventional cuvette-based techniques.

Employing this native advantage of in-fiber light-matter interaction, we have recently demonstrated a photochemically-induced functionalization of in-fiber surfaces [11]. In brief, it encompassed three phases: (1) protein passivation; (2) photo-immobilization of biotin; and (3) conjugation of streptavidin. The biotin-functionalization formed the primary bioactive surface capable of binding avidin and avidin-like molecules [12]. The subsequent binding of streptavidin thus formed the secondary bioactive surface that would enable the further binding of up to three other biotin units [13]. Considering the ease in biotinylating biomolecules [12], the construction of biomolecular assemblies on bound streptavidin would be largely facilitated. A construct, for example, is liposomes comprising biotinylated phospholipids.

Liposomes, consisting of a self-assembled bilayer of phospholipids, are closed vesicular constructs commonly used as membrane models [14], drug [15] or dye [16] delivery agents, micro-reactors [17] and bio-analytical systems [18]. A potential application, proposed in our previous work [19], is their use as optical manipulators. This was further supported by the concept of combining scatterer and laser gain medium in dye-doped crystalline [20] and polymeric [21] nanoparticles for random lasing. Specifically, it explored the potential of dye-loaded liposomes as analogues to said dye-doped nanoparticles. In our previous work, however, several drawbacks limited further studies: (1) difficulty in manipulating or altering exterior environment of liposomes without external time-consuming methods such as re-suspension after centrifugation or size-exclusion chromatography; (2) huge wastages as the platform's sample chamber required more than 0.3 ml, of which the bulk of liposomes resided outside the path of excitation light; (3) inability to continuously probe and/or excite the same population of liposomes due to the effects of diffusion over prolonged durations, which is also exacerbated by (2). On the contrary, the in-fiber surface tethering of liposomes fundamentally eliminated diffusive effects, while enabling the medium surrounding the liposomes to be easily replaced. The further choice of index guiding PCFs, offered not only broadband guidance but also surface-specificity [22], restricting light-matter interactions to sub-wavelength distances from the surface. These advantages coupled with the nanolitre volume requirements of PCFs, largely addresses the above limitations.

In this work, we first present a fluorospectroscopic means of quantifying the extent of in-fiber functionalization. This biomolecular-functionalization was achieved using our

Manuscript received August 1, 2015. This work was supported by the A*STAR SERC Advanced Optics Engineering TSRP Grant 1223600011. The first author would also like to acknowledge the scholarship sponsorship by A*STAR Graduate Academy.

Derrick Yong and Elizabeth Lee are with the Singapore Institute of Manufacturing Technology and the Division of Bioengineering, School of Chemical and Biomedical Engineering, Nanyang Technological University.

Elizabeth Lee is with the Precision Measurements Group, Singapore Institute of Manufacturing Technology.

Xia Yu is with the Precision Measurements Group, Singapore Institute of Manufacturing Technology, 71 Nanyang Drive, Singapore 638075 (e-mail: xyu@SIMTech.a-star-edu.sg).

Chi Chiu Chan is with the Division of Bioengineering, School of Chemical and Biomedical Engineering, Nanyang Technological University, 62 Nanyang Drive, Singapore 637459 (e-mail: eccchan@NTU.edu.sg).

previously demonstrated in-fiber photo-immobilization technique [11]. The method of quantification would entail a ratiometric approach in spectral analysis to in-fiber fluorescence spectroscopy [23]. Following the in-fiber surface tethering of liposomes, their fluorescent dye contents would be probed to warrant the liposomes' integrity post-surface binding. The intactness of the liposomes would reflect both their ability in retaining encapsulated contents and structural stability, implying no direct interaction with the air hole surface that would have resulted in their rupture [24]. These factors essentially determine their feasibility as analogues to dye-doped nanoparticles, where dye content and size are unvaried parameters. In brief, we report the first demonstration of an in-fiber means of tethering and exciting liposomes, via a simple and hazard-free photo-immobilization of a bioactive surface, all of which were facilitated by the inherent optofluidic properties of PCFs.

II. Methodology

A. Chemicals and Other Materials

1,2-Dipalmitoyl-sn-glycero-3-phosphocholine (DPPC) and 1,2-dipalmitoyl-sn-glycero-3-phosphoethanolamine-N-(biotinyl) (biotin-DPPE) were purchased from Avanti Polar Lipids, Inc. (Alabaster, Alabama, USA). 5(6)-Carboxyfluorescein (CF), bovine serum albumin (BSA), biotin-4-fluorescein (B4F), streptavidin (SA), Atto 488-streptavidin (AttoSA) and phosphate buffered saline at pH 7.4 (PBS) were obtained from Sigma-Aldrich (Singapore). 1 M Tris buffer at pH8.8 was purchased from 1st Base (Singapore). All other chemicals were of reagent grade.

Whatman Nucleopore track-etched polycarbonate membrane filters with pore size of 0.2 μm and PD-10 desalting columns (packed with Sephadex G-25M) were acquired from GE Healthcare (Singapore). PCFs were manufactured by Yangtze Optical Fibre and Cable Company Ltd. (Wuhan, Hubei, People's Republic of China).

B. Liposome Fabrication and Characterization

Biotinylated-liposomes encapsulating 100 mM CF (bLipo(CF)) were prepared using our earlier reported method [19], with modifications detailed as follows.

DPPC and biotin-DPPE were mixed in a molar ratio of 99:1, with each batch comprising 0.025 mg (2.66×10^{-8} mol) of biotin-DPPE and 1.975 mg (2.69×10^{-6} mol) of DPPC. In order to facilitate the fabrication process, however, the phospholipids were prepared at 4x the above-mentioned amounts – 0.1 mg biotin-DPPE to 7.9 mg DPPC. Following solvation in 6 ml of diethyl ether and 2 ml of chloroform, it was evenly aliquoted into four 2-ml tubes. Each tube was then processed according to our previously detailed method. It should be noted that after the vacuum-oven-assisted removal of the organic phase, samples could be stored under refrigeration for later use – yielding comparable results, despite having been stored for a month.

Aliquots of bLipo(CF) were diluted 400,000x in 0.32 M Tris for concentration quantification with the NanoSight LM10 system, coupled with its nanoparticle tracking analysis software. Size measurements, on the other hand, were performed using a Zetasizer Nano ZS (Malvern Instruments) at 1,000x dilution.

C. Background on Photochemistry

Several biotin-4-fluorescein (B4F) photo-immobilizations onto bovine serum albumin (BSA)-passivated surfaces have been reported on planar substrates [25, 26] and microfluidic channels [27]. This process is summarized as follows.

Prior to photo-immobilization, BSA is first passivated onto a desired surface [28, 29], where the primary driving force has been attributed to irreversible protein structural changes [30]. The subsequent B4F to BSA coupling process fundamentally involves the fluorescein (Fl) component of B4F and a Tyrosine residue (Tyr) of BSA [31], enabled by their radicalization. Following the excitation of Fl it is radicalized via electron transfer from its excited triplet state [32]:

$$S + h\nu \rightarrow S^* \text{ (absorption of light)} \quad (1)$$

$$S^* \rightarrow T^* \text{ (inter-system crossing)} \quad (2)$$

$$(T^* + T^*) \text{ or } (T^* + S) \rightarrow R + X \text{ (electron transfer)} \quad (3)$$

where S and T are the singlet and triplet ground states of Fl respectively, with * denoting their excited counterparts; R and X, represent the semi -reduced and -oxidised Fl radical (Fl•), correspondingly.

Tyr, on the other hand, is radicalized [33] by photosensitized singlet oxygen [34]:

$$T^* + {}^3O_2 \rightarrow S + {}^1O_2 \text{ (quenching)} \quad (4)$$

$$Tyr(\text{-}H) + {}^1O_2 \rightarrow Tyr\cdot + HO_2 \quad (5)$$

The subsequent radical-radical reaction results in the formation of a Tyr-Fl bond and therefore a linkage between BSA and biotin:

$$Tyr\cdot + Fl\cdot \rightarrow Tyr\text{-}Fl \quad (6)$$

D. In-fiber Photo-immobilization of Biotin

Defected-core PCFs [35] (hereon referred to as PCFs for simplicity) were cut to lengths of 105 mm and functionalized internally via our earlier described technique [11]. Adjustments were made to the said technique and elaborated in the ensuing paragraphs. All infiltrations or flushing of PCFs were performed with a customized 50 ml syringe pump, drawn at the maximum unless otherwise stated. Spectroscopic and photo-immobilization procedures were conducted using a modified version of our previously devised platform [36] (shown in Fig. 1A) – excitation input: 2.3 mW 490 nm fiber-coupled LED (Thorlabs, M490F1); spectral output acquisition: computer-linked spectrometer (Ocean Optics, Maya2000).

Prior to photo-immobilization, the air hole surfaces of PCFs were first passivated with a base layer of BSA. This was achieved via two 30 min continuous infiltrations with 2 % BSA, under 6 ml of drawn pressure. Each BSA infiltration was followed promptly by 15 min of flushing with distilled ultra-filtrated water (DIUF H_2O). 2 % BSA was prepared by dusting 10 mg of BSA into 0.5 ml of distilled ultra-filtrated

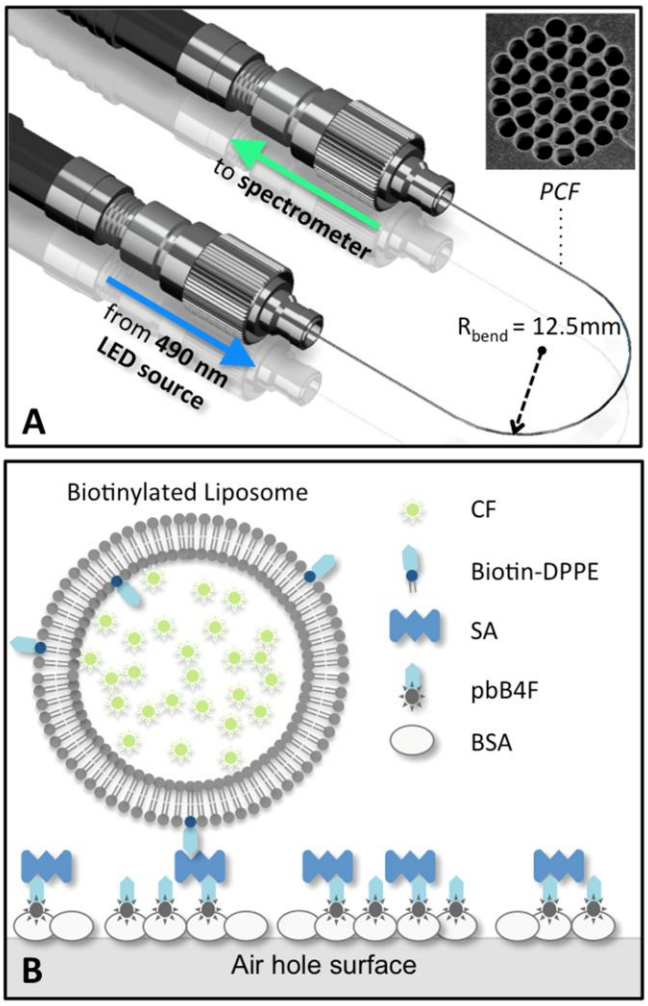

Fig. 1. (A) Configuration of platform for all in-fiber processes – 105 mm length of PCF bent at a radius of 12.5 mm coupled to an LED source (input) and a computer-linked spectrometer (output) at opposite ends. Inset: SEM Micrograph of the employed PCF's microstructure. (B) Schematics of an in-fiber surface-tethered liposome. (CF: carboxyfluorescein; SA: streptavidin; pbB4F: photobleached biotin-4-fluorescein; BSA: bovine serum albumin)

water and dissolved via gently rocking. The solution could subsequently be refrigerated and be aliquoted for usage over a week.

The primary bioactive surface was next photo-immobilized via a prolonged in-fiber excitation of B4F, creating BSA-bound photobleached B4F (BSA-pbB4F). B4F at 77.6 µM in 0.01 M PBS was infiltrated for duration of 5 min. The 10 min span of B4F photobleaching and its corresponding spectral data was subsequently facilitated via the earlier mentioned platform. Photobleaching was performed under the maximum excitation input from the fiber-coupled LED. Excess B4F was subsequently flushed with DIUF H_2O for 20 min. B4F was prepared at a concentration of 3.88 mM in 0.05 M PBS (2.5 mg/ml), allowing for prolonged storage under room temperature. Its diluted form of 77.6 µM, however, possesses a shelf life of only up to two weeks.

E. Conjugation and Quantification of (Atto 488-)Streptavidin

The successive introduction of SA or its dye-conjugated counterpart, AttoSA, generated the secondary bioactive surface (BSA-pbB4F-SA or BSA-pbB4F-AttoSA, correspondingly) capable of binding further units of biotin. SA or AttoSA was infiltrated for 5 min at 1 mg/ml (in 0.01 M PBS) concentrations. This was immediately followed by a 20 min flushing with DIUF H_2O to remove unbound SA or AttoSA. An additional 15 min of incubation under no applied pressure, with one end of the PCF remaining in the DIUF H_2O, was also performed. SA and AttoSA were aliquoted and frozen for storage, while thawed volumes were used for a maximum period of two weeks with refrigeration. Spectral data was similarly acquired, particularly for AttoSA – required for the subsequent quantification of coverage density.

Using our previously reported model for in-fiber fluorospectroscopy [23], corresponding concentrations of AttoSA ([AttoSA]) could be computed from the ratio between the intensities at the peak absorption ($\lambda_{Atto488,exc}$ = 501 nm) and emission ($\lambda_{Atto488,ems}$ = 525 nm) of Atto488 – $I(\lambda_{Atto488,ems})/I(\lambda_{Atto488,exc})$. The required inputs were: (1) an experimentally obtained reference spectrum of water-filled BSA-coated PCF, normalized to λ_{exc} (i.e. $I_0(\lambda)/I_0(\lambda_{Atto488,exc})$) and (2) fluorophore parameters from ATTO-TEC Gmbh's online database – (i) extinction coefficient, $\varepsilon(\lambda)$; (ii) fraction of fluorescence emission, $f_{Fl}(\lambda)$, at the two wavelengths of interest $f_{Fl}(\lambda_{Atto488,exc})$ = 0.00276 and $f_{Fl}(\lambda_{Atto488,ems})$ = 0.0191; (iii) quantum yield, Φ_{Fl} = 0.8.

The respective densities of surface coverage by AttoSA could then be calculated. With the assumption of a monolayer of AttoSA and each SA possessing an average of two Atto488 molecules, the coverage density (in μm^{-2}) can be approximated by:

$$coverage\ density = \frac{1}{2}\varepsilon_{Atto488}\Phi_{Fl}\,N_A\,d_p \qquad (7)$$

where d_p is the penetration depth calculated from the model (d_p = 76.46 nm) and N_A is Avogadro's constant (N_A = 6.022 x 10^{23} mol^{-1}).

F. Surface Tethering and Characterization of Liposomes

bLipo(CF) was infiltrated at a dilution of 10x for 5 min. Likewise, this was immediately flushed with 0.32 M Tris for 20 min, to remove free, non-tethered bLipo(CF). Again, the remaining bound bLipo(CF) were probed using the platform. In addition, a further 30 min duration of photobleaching under maximum excitation was performed, with the spectral data logged. The ratiometric change ($I(\lambda_{CF,ems})/I(\lambda_{CF,exc})$ where $\lambda_{CF,ems}$ = 510 nm and $\lambda_{CF,exc}$ = 490 nm) was subsequently studied over time to discern the phenomenon of photobleaching dequenching in the surface-tethered dye-loaded liposomes.

III. Results and Discussion

A. Coverage Density of Bioactive Surface

As shown in Fig. 2, the intensity ratio $I(\lambda_{Atto488,ems})/I(\lambda_{Atto488,exc})$ was calculated for each spectrum – obtained from water-filled PCFs following the conjugation of

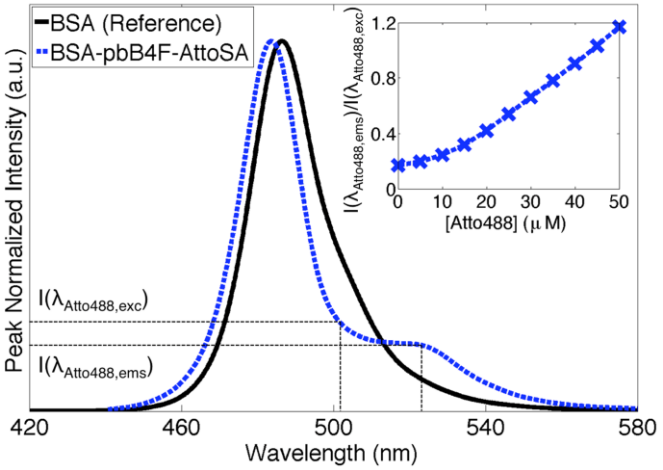

Fig. 2. Peak normalized intensities of water-filled PCFs with only a BSA coat (black solid line) and following the binding of AttoSA to BSA-bound B4F (blue dashed line). Corresponding intensities at $\lambda_{Atto488,ems}$ = 525 nm and $\lambda_{Atto488,exc}$ = 501 nm are indicated by black dotted lines. Inset: Ratiometric intensities computed from the referenced in-fiber fluoroscpectroscopy model for varying concentrations of Atto488.

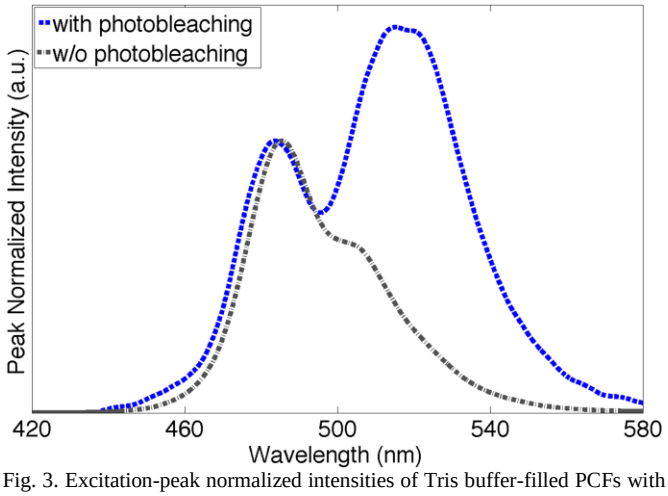

Fig. 3. Excitation-peak normalized intensities of Tris buffer-filled PCFs with its earlier infiltrated B4F photobleached (blue dotted line) – i.e. bLipo(CF) tethered to the discussed bioactive surface or simply, BSA-pbB4F-SA-bLipo(CF) – and without B4F photobleaching (grey dotted-dashed line).

AttoSA to a BSA-bound biotin layer (BSA-pbB4F-AttoSA). It should be noted here, and in all subsequently presented spectra, that the bulk of the spectrum corresponds to the remaining 490nm LED excitation input, while any spectral features on the right generally reflects any fluorescence emission collected.

From the model-computed intensity ratios (Fig. 2(inset)), the corresponding [Atto488] values were acquired. With [Atto488], the extent of coverage by AttoSA was calculated from Eq. (7). From a triplicate repetition of the in-fiber photo-immobilization process, a coverage density of 616 ± 59 μm^{-2} was obtained from an intensity ratio of 0.610 ± 0.077. Extending the duration of photobleaching to 15 min was observed to yield only a 4 % increment in coverage density. This was in contrast to a 19 % increment obtained by increasing the photobleaching duration from 5 to 10 min. For reasons of efficiency and repeatability, a 10 min span of photobleaching was deemed optimal.

The computed coverage, however, comprised not only the desired biotin-bound AttoSA, but also included non-specifically bound AttoSA. The primary contributor being AttoSA's attachment to the in-fiber silica surfaces [37] not covered by BSA. Using the same method of quantification, the extent of non-specific coverage by AttoSA was similarly calculated. For each of the triplicate repetition, a control was concurrently performed, where all reagents and conditions were one and the same, with the only difference being the absence of an exposure to the LED excitation – i.e. the B4F infiltrated PCF was allowed to sit for 10 min in air, while its counterpart underwent photobleaching. These were calculated to possess a coverage density of 449 ± 31 μm^{-2} from an intensity ratio of 0.415 ± 0.032. Despite this relatively significant amount of non-specifically bound AttoSA, their effectiveness in functioning as a bioactive surface is severely hindered by: (1) a one to five order reduction in binding affinity to biotin upon a prior direct surface attachment of SA [38, 39]; (2) steric hindrance due to (i) SA's "buried" position amongst the base layer of BSA and (ii) a lost of biotin binding sites at the interface between SA and adjacent BSA; (3) a relatively weaker attachment of SA due to its potentially smaller footprint (SA native profile: 4.5 nm x 4.5 nm x 5 nm) in contrast to its BSA-bound counterparts (BSA native profile: 4 nm x 4 nm x 14 nm), resulting in easier dissociation under continuous shear forces. Hence, it becomes appropriate to assume minimal contributions by the non-specifically bound AttoSA or SA in the provision of enduring and stable biotin binding sites for the subsequent conjugation of biotinylated liposomes. This assumption is further substantiated by the evident spectral difference depicted in the following section discussing the characterization of surface-tethered liposomes.

B. Characterization of Surface-Tethered Liposomes

bLipo(CF), sized at 224.73 ± 15.96 nm, were infiltrated at a concentration of (1.10 ± 0.22) x 10^{13} ml^{-1}. Following the removal of excess unbound bLipo(CF), the resultant spectra of in-fiber bioactive-surface-tethered bLipo(CF) (BSA-pbB4F-SA-bLipo(CF), illustrated in Fig. 1B) were acquired and contrasted with its control (without B4F photobleaching) as shown in Fig. 3.

An obvious distinction between the two spectra was noted, where the significance of the spectra's right ends corresponded to the extent of fluorescence emission by CF. The significant emission peak depicted by the blue dotted plot in Fig. 3, implied the presence of CF, which in turn, was indicative of the existence of bLipo(CF). In contrast, the weak emission or "shoulder" observed in its non-photobleached counterpart's spectrum, could be attributed to the earlier discussed non-specific binding of SA. Although this did result in the consequent binding of bLipo(CF), the weak "shoulder" corresponded to an insignificant amount, relative to that observed in the case with specifically bound SA. However, this largely conflicted with the calculated coverage density of non-specifically bound SA, which was deemed to comprise more than three-quarters of the total bound (both specific and

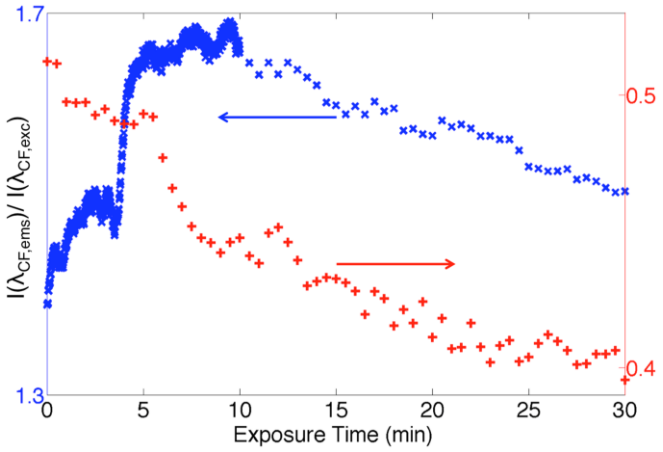

Fig. 4. Evolution of $I(\lambda_{CF,ems})/I(\lambda_{CF,exc})$ over the duration of photobleaching for surface-tethered bLipo(CF) (blue 'x's and left y-axis) and surface-tethered heat-treated bLipo(CF) (red '+'s and right y-axis).

non-specific) SA. Hence, as discussed in the earlier section, results in this section do support the hypothesis that non-specifically bound SA possesses hindered functionalities. Similarly, the study was performed in triplicates, yielding a $I(\lambda_{CF,ems})/I(\lambda_{CF,exc})$ of 1.405 ± 0.116 and 0.790 ± 0.293 for BSA-pbB4F-SA-bLipo(CF) and the control respectively. It was however not possible to quantify the concentration of surface-tethered bLipo(CF) in this case, as the model does not account for the effects of concentration self-quenching [40] – present in the fabricated dye-loaded liposomes.

On the other hand, a previously reported counterintuitive phenomenon – photobleaching dequenching [19] – was employed in verifying the liposomal retention of dye at self-quenching concentrations following surface attachment. This served to determine the structural integrity and consequent encapsulation stability of the dye-loaded liposomes. From the ratiometric intensity change over the span of photobleaching (shown in Fig. 4 by blue 'x's), an increasing prominence of the fluorescence emission was observed for up to the first 10 min. This behaviour, was very much contrary to the typical photobleaching profile – a negative exponential function [32]. Briefly, dequenching was described as a result of reduced self-quenching effects within the bLipo(CF). This reduction was effected by the photobleaching of encapsulated CF, decreasing the amount of viable CF capable of participating in self-quenching effects. In contrast, a similar study was conducted with an identically prepared PCF, where the only variation was a prior heating of the bLipo(CF). The heat-induced leakage of bLipo(CF)'s contents, drastically reduces the encapsulated CF concentration and eventually resulted in an elimination of the self-quenching effect. Photobleaching these heat-treated bLipo(CF) would thus lead to no observable dequenching, evident in the continuous decrease exhibited by the red '+'s in Fig. 4.

Similar to the two dequenching phases examined in our earlier work [19], successive dequenchings was likewise observed here. From Fig. 4 (blue 'x's), two broad peaking events were observed, the first occurring between 0 and 4 min, followed promptly by a second that spanned a longer additional 6 min. Such events were attributed to the inhomogeneous-manner in which photobleaching proceeded within the liposome-encapsulated volumes. This was due to increasing "shielding", by excitation-proximal CF, towards the interior of the surface-tethered liposomes as well as the intra-liposomal diffusion of CF. In brief, photobleaching first occurred for the encapsulated CF closest to the PCF air hole surface, reducing the self-quenching effects in the immediate proximity of said photobleached CF. This continued until the effects of photobleaching eventually outweighed dequenching, resulting in the first peaking event. The subsequent dequenching, on the other hand, was more significant and persistent. The former was a result of a larger pool of self-quenched CF achieving a dequenched state as diffusive effects took prominence over the originally dominating photobleaching – due to more efficient "shielding" of CF residing further within the liposomes. Similarly, the latter, observed as gradual plateauing between 5 and 10 min of exposure, could be ascribed to diffusion from the remaining volume of encapsulated CF (outside the penetration depth). In this case of surface-tethered liposomes, the BSA-to-encapsulated-CF distance was estimated to be ~ 8.3 nm (BSA layer: 2.4 nm [41]; biotinylated phospholipid bilayer with bound SA: 5.9 nm [42]; SA-bound biotin: negligible [13]), yielding an estimated excitation penetration depth that reached only up to a third of the internal liposomal volume, substantiating an ample supply of self-quenched CF. Eventually, this resistance too succumbs, as the effects of photobleaching returns to dominance over diffusion. These successive dequenching events were likewise observed in the remainder of the triplicate repetition – both of which had exhibited dequenching lasting the first 8 to 10 min of exposure but had varied spans (1 and 5 min) for the first occurrence, possibly due to variations in concentrations of bound bLipo(CF).

IV. Conclusion

Surface tethering and fluorescence spectroscopy of liposomes were, for the first time, achieved within the same length of PCF. These were enabled by a photo-immobilized bioactive surface, comprising a base layer of passivated BSA with bound B4F. Biotinylated liposomes were then attached via the sandwiching of a SA unit. In addition, quantification of the SA coverage density was performed using its dye-conjugated counterpart, via means of in-fiber fluorospectroscopy. Despite yielding a significant quantity of non-specifically bound SA, the spectral results of subsequently bound dye-loaded liposomes substantiated its negligibility with respect to consequent non-specifically bound liposomes. Lastly, the liposomal integrity post surface tethering was uniquely verified through the observation of photobleaching dequenching – a phenomenon manifesting only in liposomes encapsulating self-quenching concentrations of dye. This implied minimal leakage of liposomal contents upon tethering, essential to the function of dye-loaded liposomes as analogues to dye-doped nanoparticles. Additionally, these surface-bound liposomes could also serve as cell phantoms for the study of membrane permeability upon interaction of various compounds or particles. More

immediately, however, PCFs with tethered liposomes could function as platforms for the study of membrane permeability via the measurement of dye release; or they could even be used in capillary electrophoresis [43] for the characterization of membrane interactions.

In summary, in-fiber light-matter interactions enabled not only the immobilization of liposomes but also the subsequent optical excitation and detection of liposomal content. These, together with the supported fluidics, show potential in applying liposome-integrated PCFs as bio-integrated photonic devices.

REFERENCES

[1] P. Russell, "Photonic crystal fibers," *Science*, vol. 299, pp. 358-362, 2003.

[2] J. C. Knight, "Photonic crystal fibres," *Nature*, vol. 424, pp. 847-851, 2003.

[3] O. Frazão, J. L. Santos, F. M. Araújo, and L. A. Ferreira, "Optical sensing with photonic crystal fibers," *Laser & Photonics Reviews*, vol. 2, pp. 449-459, 2008.

[4] A. S. J. Cerqueira, "Recent progress and novel applications of photonic crystal fibers," *Reports on Progress in Physics*, vol. 73, p. 024401, 2010.

[5] A. M. Cubillas, S. Unterkofler, T. G. Euser, B. J. M. Etzold, A. C. Jones, P. J. Sadler, *et al.*, "Photonic crystal fibres for chemical sensing and photochemistry," *Chemical Society Reviews*, vol. 42, pp. 8629-8648, 2013.

[6] F. Tian, S. Sukhishvili, and H. Du, "Photonic Crystal Fiber as a Lab-in-Fiber Optofluidic Platform," in *Lab-on-Fiber Technology*. vol. 56, A. Cusano, M. Consales, A. Crescitelli, and A. Ricciardi, Eds., ed: Springer International Publishing, 2015, pp. 315-334.

[7] J. S. Y. Chen, T. G. Euser, N. J. Farrer, P. J. Sadler, M. Scharrer, and P. S. J. Russell, "Photochemistry in Photonic Crystal Fiber Nanoreactors," *Chemistry – A European Journal*, vol. 16, pp. 5607-5612, 2010.

[8] G. O. S. Williams, J. S. Y. Chen, T. G. Euser, P. S. J. Russell, and A. C. Jones, "Photonic crystal fibre as an optofluidic reactor for the measurement of photochemical kinetics with sub-picomole sensitivity," *Lab on a Chip*, vol. 12, pp. 3356-3361, 2012.

[9] S. Unterkofler, R. J. McQuitty, T. G. Euser, N. J. Farrer, P. J. Sadler, and P. S. J. Russell, "Microfluidic integration of photonic crystal fibers for online photochemical reaction analysis," *Optics Letters*, vol. 37, pp. 1952-1954, 2012.

[10] M. Schmidt, A. M. Cubillas, N. Taccardi, T. G. Euser, T. Cremer, F. Maier, *et al.*, "Chemical and (Photo)-Catalytical Transformations in Photonic Crystal Fibers," *ChemCatChem*, vol. 5, pp. 641-650, 2013.

[11] E. Lee, D. Yong, X. Yu, H. Li, and C. C. Chan, "In-fiber photo-immobilization of a bioactive surface," *Journal of Biomedical Optics*, vol. 19, p. 120502, 2014.

[12] R. J. McMahon, *Avidin-Biotin Interactions: Methods and Applications* vol. 418: Humana Press, 2008.

[13] P. C. Weber, D. H. Ohlendorf, J. J. Wendoloski, and F. R. Salemme, "Structural origins of high-affinity biotin binding to streptavidin," *Science*, vol. 243, pp. 85-88, 1989.

[14] M. Masserini, P. Palestini, M. Pitto, V. Chigorno, and S. Sonnino, "Preparation and Use of Liposomes for the Study of Sphingolipid Segregation in Membrane Model Systems," in *Liposome Methods and Protocols*. vol. 199, S. Basu and M. Basu, Eds., ed: Humana Press, 2002, pp. 17-27.

[15] J. A. Zasadzinski, B. Wong, N. Forbes, G. Braun, and G. Wu, "Novel methods of enhanced retention in and rapid, targeted release from liposomes," *Current Opinion in Colloid Interface Science*, vol. 16, pp. 203-214, 2011.

[16] M. R. Niesman, B. Khoobehi, and G. A. Peyman, "Encapsulation of sodium fluorescein for dye release studies," *Investigative Ophthalmology & Visual Science*, vol. 33, pp. 2113-9, 1992.

[17] R. Genç, G. Clergeaud, M. Ortiz, and C. K. O'Sullivan, "Green Synthesis of Gold Nanoparticles Using Glycerol-Incorporated Nanosized Liposomes," *Langmuir*, vol. 27, pp. 10894-10900, 2011.

[18] K. A. Edwards, O. R. Bolduc, and A. J. Baeumner, "Miniaturized bioanalytical systems: enhanced performance through liposomes," *Current Opinion in Chemical Biology*, vol. 16, pp. 444-452, 2012.

[19] D. Yong, E. Lee, X. Yu, and C. C. Chan, "Two-Phase Photobleaching Dequenching in Dye-Loaded Liposomes," *Selected Topics in Quantum Electronics, IEEE Journal of*, vol. 20, pp. 213-220, 2014.

[20] S. GarcÌa-Revilla, J. Fern·ndez, M. A. Illarramendi, B. GarcÌa-Ramiro, R. Balda, H. Cui, *et al.*, "Ultrafast random laser emission in a dye-doped silica gel powder," *Optics Express*, vol. 16, pp. 12251-12263, 2008.

[21] V. Martín, J. Bañuelos, E. Enciso, I. n. i. L. p. Arbeloa, A. n. Costela, and I. García-Moreno, "Photophysical and Lasing Properties of Rhodamine 6G Confined in Polymeric Nanoparticles," *The Journal of Physical Chemistry C*, vol. 115, pp. 3926-3933, 2011.

[22] J. C. Knight, T. A. Birks, P. S. J. Russell, and D. M. Atkin, "All-silica single-mode optical fiber with photonic crystal cladding," *Optics Letters*, vol. 21, pp. 1547-1549, 1996.

[23] D. Yong, E. Lee, X. Yu, and C. C. Chan, "In-fiber fluorospectroscopy based on a spectral decomposition method," *Optics Express*, vol. 22, pp. 23640-23651, 2014.

[24] P. S. Cremer and S. G. Boxer, "Formation and Spreading of Lipid Bilayers on Planar Glass Supports," *The Journal of Physical Chemistry B*, vol. 103, pp. 2554-2559, 1999.

[25] M. A. Holden and P. S. Cremer, "Light Activated Patterning of Dye-Labeled Molecules on Surfaces," *Journal of the American Chemical Society*, vol. 125, pp. 8074-8075, 2003.

[26] J. M. Belisle, J. P. Correia, P. W. Wiseman, T. E. Kennedy, and S. Costantino, "Patterning protein concentration using laser-assisted adsorption by photobleaching, LAPAP," *Lab on a Chip*, vol. 8, pp. 2164-2167, 2008.

[27] M. A. Holden, S.-Y. Jung, and P. S. Cremer, "Patterning Enzymes Inside Microfluidic Channels via Photoattachment Chemistry," *Analytical Chemistry*, vol. 76, pp. 1838-1843, 2004.

[28] K. Nakanishi, T. Sakiyama, and K. Imamura, "On the adsorption of proteins on solid surfaces, a common but very complicated phenomenon," *Journal of Bioscience and Bioengineering*, vol. 91, pp. 233-244, 2001.

[29] B. Sweryda-Krawiec, H. Devaraj, G. Jacob, and J. J. Hickman, "A New Interpretation of Serum Albumin Surface Passivation," *Langmuir*, vol. 20, pp. 2054-2056, 2004.

[30] W. Norde, "Adsorption of proteins from solution at the solid-liquid interface," *Advances in Colloid and Interface Science*, vol. 25, pp. 267-340, 1986.

[31] J. Brandt, M. Fredriksson, and L. O. Andersson, "Coupling of dyes to biopolymers by sensitized photooxidation. Affinity labeling of a binding site in bovine serum albumin," *Biochemistry*, vol. 13, pp. 4758-4764, 1974.

[32] L. Song, E. J. Hennink, I. T. Young, and H. J. Tanke, "Photobleaching kinetics of fluorescein in quantitative fluorescence microscopy," *Biophysical Journal*, vol. 68, pp. 2588-2600, 1995.

[33] A. Wright, W. A. Bubb, C. L. Hawkins, and M. J. Davies, "Singlet Oxygen–mediated Protein Oxidation: Evidence for the Formation of Reactive Side Chain Peroxides on Tyrosine Residues," *Photochemistry and Photobiology*, vol. 76, pp. 35-46, 2002.

[34] M. C. DeRosa and R. J. Crutchley, "Photosensitized singlet oxygen and its applications," *Coordination Chemistry Reviews*, vol. 233–234, pp. 351-371, 11/1/ 2002.

[35] X. Yu, Y. Sun, G. B. Ren, P. Shum, N. Q. Ngo, and Y. C. Kwok, "Evanescent Field Absorption Sensor Using a Pure-Silica Defected-Core Photonic Crystal Fiber," *Photonics Technology Letters, IEEE*, vol. 20, pp. 336-338, 2008.

[36] D. Yong, W. L. Ng, X. Yu, and C. C. Chan, "A compact opto-fluidic platform for chemical sensing with photonic crystal fibers," *Sensors and Actuators A: Physical*, vol. 191, pp. 22-26, 2013.

[37] M. L. Korwin-Edson, A. G. Clare, M. M. Hall, and A. Goldstein, "Biospecificity of glass surfaces: streptavidin attachment to silica," *Journal of Non-Crystalline Solids*, vol. 349, pp. 260-266, 2004.

[38] K. Fujita and J. Silver, "Surprising lability of biotin-streptavidin bond during transcription of biotinylated DNA bound to

paramagnetic streptavidin beads," *BioTechniques*, vol. 14, pp. 608-617, 1993.
[39] S.-C. Huang, M. D. Stump, R. Weiss, and K. D. Caldwell, "Binding of Biotinylated DNA to Streptavidin-Coated Polystyrene Latex: Effects of Chain Length and Particle Size," *Analytical Biochemistry*, vol. 237, pp. 115-122, 1996.
[40] R. F. Chen and J. R. Knutson, "Mechanism of fluorescence concentration quenching of carboxyfluorescein in liposomes: Energy transfer to nonfluorescent dimers," *Analytical Biochemistry*, vol. 172, pp. 61-77, 1988.
[41] E. H. Tronic, "Surface Analysis of Adsorbed Proteins: A Multi-Technique Approach to Characterize Surface Structure," University of Washington, 2012.
[42] A. Schmidt, J. Spinke, T. Bayerl, E. Sackmann, and W. Knoll, "Streptavidin binding to biotinylated lipid layers on solid supports. A neutron reflection and surface plasmon optical study," *Biophysical Journal*, vol. 63, pp. 1385-1392, 1992.
[43] R. L. Owen, J. K. Strasters, and E. D. Breyer, "Lipid vesicles in capillary electrophoretic techniques: Characterization of structural properties and associated membrane-molecule interactions," *ELECTROPHORESIS*, vol. 26, pp. 735-751, 2005.

Derrick Yong received his B. Eng. in Bioengineering from the School of Chemical and Biomedical Engineering (SCBE) at Nanyang Technological University (NTU), Singapore. He is currently an Attachment Student in Singapore Institute of Manufacturing Technology (SIMTech), Agency for Science Technology and Research (A*STAR) and a Ph. D Candidate in SCBE, NTU. His research interests include optical fiber devices, in-fiber light-matter interactions and biophotonics.

Elizabeth Lee received her B. Eng. from SCBE, NTU, Singapore. She is currently a Research Engineer in SIMTech, A*STAR.

Xia Yu received her B. Eng. and Ph.D. degrees from the School of Electrical and Electronic Engineering (EEE), NTU, Singapore, in 2003 and 2007 respectively. Since 2008, she has been working as a scientist in the Precision Measurements Group of SIMTech, A*STAR. Her current research interests include photonic crystal fibers, fiber lasers and non-linear optics.

Chi Chiu Chan received his B. Eng. and Ph.D from the Department of Electrical Engineering, the Hong Kong Polytechnic University in 1996 and 2000 respectively. From 2000 to 2003, he was a Postdoctoral Fellow in the Department of Electrical Engineering of the Hong Kong Polytechnic University. Currently, he is an Associate Professor in SCBE, NTU. His research areas are optical fiber sensing system, fiber Bragg grating device, fiber optics chemical sensors, photonics crystal fiber biosensor, digital signal processing, such as artificial neural network, fuzzy logic, genetic algorithm, wavelet, etc., on smart structures, fiber optics chemical and biomedical sensing areas. His accomplishment in these areas is demonstrated in his 200 international publications.